Center for Advanced Materials

CAM

Presented at the 5th International Aluminum-Lithium Conference, Williamsburg, VA, March 28–31, 1989, and to be published in the Proceedings

The Strength-Toughness Relationship at Cryogenic Temperatures in Aluminum-Lithium Alloy Plate

J. Glazer and J.W. Morris, Jr.

March 1989

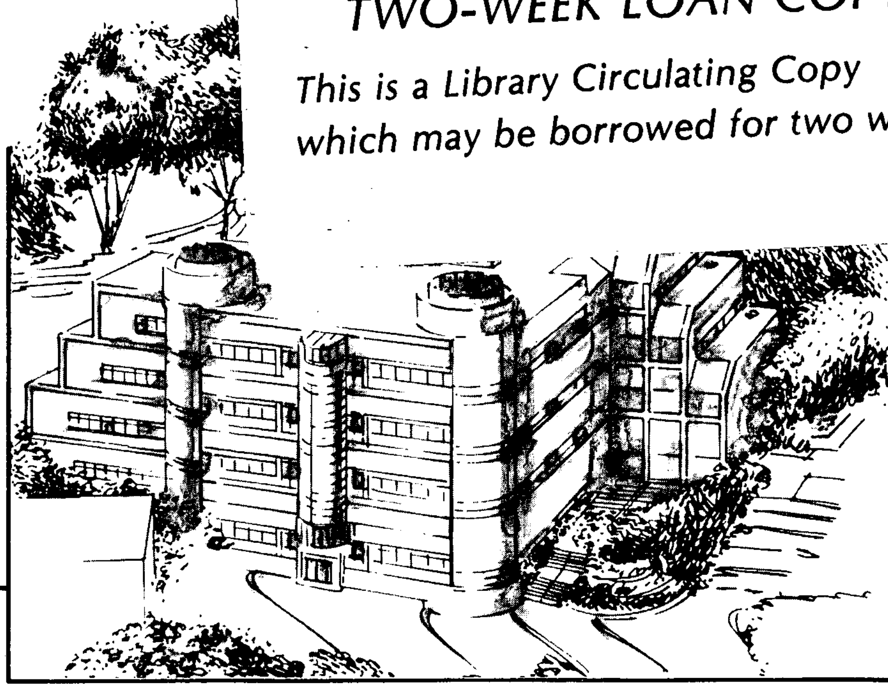

Materials and Chemical Sciences Division

Lawrence Berkeley Laboratory • University of California

ONE CYCLOTRON ROAD, BERKELEY, CA 94720 • (415) 486-4755

Prepared for the U.S. Department of Energy under Contract DE-AC03-76SF00098

DISCLAIMER

LBL-26653

THE STRENGTH-TOUGHNESS RELATIONSHIP AT CRYOGENIC TEMPERATURES IN ALUMINUM-LITHIUM ALLOY PLATE

J. Glazer and J.W. Morris, Jr.

Department of Materials Science and Mineral Engineering,
University of California

and

Center for Advanced Materials
Materials and Chemical Sciences Division
Lawrence Berkeley Laboratory
1 Cyclotron Road
Berkeley, California 94720

March, 1989

This study was funded by the Director, Office of Energy Research, Office of Basic Energy Science, Material Sciences Division of the U.S. Department of Energy under Contract No. DE-AC03-76SF00098. J. Glazer was supported by an AT&T Bell Laboratories PhD Scholarship.

The Strength-Toughness Relationship at Cryogenic Temperatures in Aluminum-Lithium Alloy Plate

J. Glazer and J.W. Morris, Jr.

Center for Advanced Materials, Lawrence Berkeley Laboratory and
Department of Materials Science and Mineral Engineering,
University of California at Berkeley

Both 2090-T81 and 2091-T8 plate display increasing strength, fracture toughness and elongation with decreasing test temperature for some low temperature regimes, test orientations and tempers. The relation between these properties and the fracture behavior is explored in this study in an attempt to elucidate the source of the increase in toughness observed at low temperature. Various alternate mechanisms are explored, including the influences of crack-dividing intergranular splitting and increased plastic deformation on the work of fracture. It is concluded that when the primary fracture mode is unchanged, the best correlation with experiment is achieved by relating the toughness and the deformation properties of the material.

INTRODUCTION

The cryogenic mechanical properties of aluminum-lithium alloys have attracted considerable interest in the last few years. Their low density, weldability, relatively high strength and tendency to show improved properties at low temperatures make them candidate alloys for large tanks for liquid cryogenic fuels (1). Examples of systems that use or are projected to use such tanks are the space shuttle, the National Aerospace Plane (NASP) and the Advanced Launch System (ALS).

Although existing commercial aluminum-lithium alloys, particularly 2090 (2-7), often have cryogenic properties superior to their room temperature mechanical properties, these alloys were not designed for cryogenic service and the mechanisms that control their cryogenic behavior are not well understood. Toughness improvements with decreasing temperature are not unique to aluminum-lithium alloys and have been observed in several aluminum alloys and in other fcc materials. Nonetheless, while the cryogenic properties of many aluminum alloys have been measured, there have been few mechanistically oriented studies, even of those alloys such as 2219 that are currently used for cryogenic service (1).

This paper presents the results of a study of the tensile and fracture toughness behavior between 4 and 300 K of two commercial aluminum-lithium alloys. The goal of the work is to provide a consistent mechanistic interpretation for the observed behavior. Three previously proposed explanations for improved fracture toughness at low temperature are considered: 1) the fracture mode; 2) crack-dividing splitting that lowers the triaxiality of the nominally plane strain stress state; and 3) the influence of strength and strain-to-failure on the work of fracture.

EXPERIMENTAL PROCEDURES

Materials. The properties of 2090-T81 and 2091-T8 plate were investigated. The 2090 plate was received in the form of 12.5 mm (0.5 in) plate in the -T8 condition (2). The 2091 plate was received in the form of 38.1 mm (1.5 in) plate in the as-fabricated condition. The -T8 processing consisted of: solution treatment at 530°C for 1 hour of 16 mm slabs centered at T/4 (quarter-thickness), quench into 65°C water, rolling 6% immediately after quenching and aging to peak strength at 190°C for 24 hours. Experimental details are given in ref. 6.

Microstructures. Both materials had an unrecrystallized, elongated grain structure. The mean grain size of the 2090 was approximately 2200 x 400 x 25 μm. The 2091 grains were slightly less elongated; their average size was 1400 x 400 x 70 μm. A few small particles remained in the 2091 microstructure after solution treatment.

Mechanical testing. Mechanical testing was performed using standard techniques. All quoted values are averages of two or, occasionally, three tests. Details of tensile specimen design and testing technique have been given previously (2,6). Satisfaction of the necking criterion was checked using the procedure described in ref. 7. Short-transverse (ST) tensile specimens from the 12.5 mm thick 2090 plate were manufactured by electron-beam welding grip sections to the plate. These specimens had a gauge length of 4 mm and a gauge width of 1.3 mm. Due to the small dimensions elongation was not measured, but was less than 4% at all temperatures. Fracture toughness was measured by determining J_{Ic} for standard compact tension specimens with W=2.0 according to ASTM E813 (1981 standard for 2090; 1987 standard for 2091) using the single-specimen compliance technique. $K_{Ic}(J)$ values were calculated using the value of the elastic modulus E at the test temperature (8). Since values for E as function of temperature are unknown for 2091, the values for 2090 were also used for 2091. This procedure is reasonable since the lithium contents of the two alloys are similar.

Fracture morphology. Intergranular splitting was characterized by examining the fracture profile perpendicular to the crack front within 2 mm of the fatigue precrack. The splitting was quantified by digitizing the endpoints of each split from a series of optical micrographs

TABLE 1 - Mechanical Properties of 2090-T81 at Various Test Temperatures.
(TYS = Tensile Yield Strength; UTS = Ultimate Tensile Strength)

Test Direction	Test Temp. (K)	E (GPa)	TYS (MPa)	UTS (MPa)	% Elongation Uniform	Total	KIc(J) (MPa$\sqrt{m}$)
L / L-T	300	78.3	535	565	5.0	11.0	34
	77	86.9	600	715	7.0	13.5	57
	4	87.6	615	820	17.0	17.5	72
T / T-L	300	78.3	535	565	4.0	5.5	25
	77	86.9	625	695	5.0	5.5	37
	4	87.6	705	815	6.5	6.5	43

Note. K_{Ic}(J) have been calculated using the correct elastic modulus E at each test temperature. They differ slightly from values in ref. 2 computed using the modulus at 300 K.

of the entire 12.5 mm thickness. This information was used to compute histograms and mean values for the depth and spacing of the splits.

MECHANICAL PROPERTIES

2090-T81. The mechanical properties of 2090-T81 at T/2 in the plane of the plate are summarized in Table I and Figure 1. The yield strength, ultimate tensile strength, elongation and fracture toughness all increase with decreasing temperature. Although little or no necking was observed in the tensile specimens, it is believed

that they all failed at or slightly beyond the point at which uniform elongation is unstable ($d\sigma/d\varepsilon = \sigma$, where σ and ε are the true stress and strain, respectively). It has been verified that this criterion is satisfied for L-oriented specimens at T/4. Thus the uniform elongation is determined chiefly by the strain hardening rate, which increases with decreasing temperature (7). The yield strength and fracture strength in the ST direction also increase with decreasing temperature (see Figure 2). This result is perhaps surprising; Dew-Hughes et al. (9) found that the ST fracture strength decreased with decreasing temperature in 8090.

It should be noted that the mechanical properties vary considerably through the plate thickness. The strengths reported here at T/2 are ~ 15% higher than those measured at T/4 (7). The tensile elongation and its response to temperature also vary through the thickness. The ST specimens test the through-thickness properties of the plate and hence represent minimum values. The fracture toughness measurements test the entire thickness

TABLE 2 - Mechanical Properties of 2091-T8 at Various Test Temperatures.

Test Direction	Test Temp. (K)	TYS (MPa)	UTS (MPa)	% Elongation Uniform	% Elongation Total	KIc(J) (MPa$\sqrt{m}$)
L / L-T	300	440	480	5	6	24
	200	460	495	7	7	32
	77	495	565	10	10	32
	4	550	630	7	7	32
LT / T-L	300	430	465	2	2	22
	200	445	495	4	4	28
	77	485	535	3	3	33
	4	510	585	3	3	38

in parallel and represent average values. This variability significantly complicates interpreting the results.

2091-T8. The mechanical properties of 2091-T8 are summarized in Table 2 and Figure 1. The most important result is that while the yield and ultimate tensile strength increase monotonically with decreasing temperature, the elongation and toughness do not. In both orientations there is a peak in elongation between room temperature and 4 K. The peak in L elongation is associated with a peak in L-T fracture toughness. However, there is no corresponding peak in the T-L fracture toughness. Comparison of the strain hardening rate to the true stress shows that the low elongations are the result of premature failures; in the L orientation, the 300 and 200 K specimens necked and the 77 K specimen failed at instability; in the LT orientation only the 200 K specimens clearly failed beyond instability. In spite of the lower strength of this alloy, the strain hardening rates were lower than those measured for 2090-T81 (6).

FRACTURE BEHAVIOR

Fracture mode. With one important exception the primary fracture mode was unaffected by the test temperature. The constancy in 2090-T8 has already been reported (2-4,7). The fracture mode of 2091-T8 has a woody appearance similar to that seen for 2090-T81, especially in tension. No mode change was observed in tension or in the L-T fracture specimens. However, the fracture mode in the T-L orientation did change with temperature; cleavage-like flat facets were observed at room temperature, while ductile dimples are present at 77 and 4 K (see Figure 3). The source of this transition is not currently understood. The macroscopic 2090 ST tensile failure mode appears similar to that observed for 8090 (9).

Intergranular splitting. All J_{Ic} specimens had intergranular splits along the long-transverse planes. The mean spacing between splits as a function of test temperature and minimum split depth is shown in Figure 4 for both alloys in the L-T orientation. The equivalent plots for T-L specimens show the same trends, although the splits are further apart and not as deep. The average values for 2090 L-T at 300 and 77 K for splits deeper than 0.4 mm are 3.1 mm and 1.4 mm, respectively, in good agreement with values quoted by Rao et al. (3 and < 1 mm) (10). The corresponding spacing at 4 K is greater, 2.1 mm. There are many shallower splits; if these are included the split spacing decreases, but their effect on the toughness should be small. The splits in the 2091 specimens were slightly more frequent and tended to be deeper. In contrast to the behavior of 2090, the split spacing decreased monotonically with decreasing temperature for all minimum split depths examined.

Transverse splitting in the strain field of a growing crack was investigated by sectioning a 2090 specimen in which the crack was allowed to propagate a short distance at 77 K (see Figure 5). The material is split well ahead of the current crack front. The split distance compares reasonably with the distance ahead of the crack at which the through-thickness stress corresponding to the applied stress intensity is predicted to exceed the failure stress in the ST direction, which also corresponds roughly to the size of the plastic zone. The longer splits are more regularly spaced; their spacing corresponds to the mean spacing of the deep splits in the fracture profile.

THE EFFECT OF TEMPERATURE ON FRACTURE TOUGHNESS

Several mechanistic theories of the effect of temperature on fracture toughness in these alloys are described below. They are not mutually exclusive. Strain hardening and intergranular delamination are probably closely related. Texture and grain shape are almost certainly important. Nor is the list complete, although the continued improvement in fracture toughness observed between 77 and 4 K would appear to rule out the "liquid phase" model proposed by Webster (1, 11)

Fracture mode. The most obvious source of a change in fracture toughness is a shift from a ductile to a brittle fracture mode. Neither 2090-T81 nor 2091-T8 in the L-T orientation display a change of primary fracture mode. Thus there must be other factors that explain the change in fracture toughness. However, in superplastic 2090-T6 (12) a transition from ductile shear failure at 300 K to intergranular cleavage at 4 K is observed. This transition is associated with a decrease in apparent toughness (as measured by unit propagation energy) with decreasing temperature, although the tensile elongation increases. The reverse transition is observed in 2091 T-L oriented fracture specimens. In this orientation 2091 does show a mode transition; the fracture appears more ductile at lower temperatures. As an apparent consequence the toughness increases even though the ductility decreases. For both 2090 orientations and 2091 L-T, the fracture mode is constant and the tensile elongation and fracture toughness correlate.

Crack-dividing splitting. It is well known that intergranular splits that divide a thick specimen into thin laminates can raise the apparent fracture toughness by relieving some of the stress triaxiality present in a nominally plane strain fracture toughness specimen (13). Conversely, if a material is relatively weak in the short transverse direction a high fracture toughness will induce splitting because of the large through-thickness stress at the crack tip. Hence transverse splitting may be either a cause of high fracture toughness or a consequence of it, and detailed studies are necessary to elucidate its role. Several investigators have suggested that increased splitting can explain the observed improvement in low temperature fracture toughness in 2090-T81 (3,4,10). The results of this investigation seem to establish that transverse splitting is not the dominant cause of the toughness increase at low temperature. This conclusion is supported by three main considerations.

First, there is no consistent experimental correlation between the split spacing and the fracture toughness. In three of the four cases studied here the correlation is reversed for at least part of the temperature range; increased split spacing is associated with increased toughness. The fracture toughness of 2090-T81 L-T and T-L increases between 77 and 4 K, but the spacing between deep splits increases. The fracture toughness of 2091-T8 L-T does not increase between 200 and 4 K, but the split spacing decreases monotonically with temperature. In 2091-T8 T-L, the decrease in split spacing with temperature is monotonic and greater than that observed for 2090. However, while the toughness does increase, the increase is considerably less than in 2090 despite a beneficial change in the microscopic fracture mode. The lack of a consistent correlation between the amount of splitting and toughness has also been noted by Webster (11).

Second, there is no clear theoretical reason to expect a monotonic dependence of the toughness on the split spacing for tests done at different temperatures. The available models consider the toughness of laminates of independent plates, which certainly overestimates the effect of transverse splitting in the immediate vicinity of the crack tip. The elevation of the toughness of the lamina over K_{Ic} must in turn be modeled as a function of their thickness (14). The models include a number of material properties that are unknown for Al-Li alloys and difficult or impossible to measure. Depending on the relative variation of the known and unknown material properties with temperature, the estimated toughness may either increase or decrease when both the split spacing and the temperature are changed.

Third, if delamination becomes more difficult at low temperature then the increased number of splits at low temperature may be ascribed to the increased stress intensity. This possibility can be assessed for 2090. Although the S-T fracture toughness is low and decreases with temperature (4), there are no introduced cracks on the S-T fracture planes and estimates based on the presence of an internal penny-shaped crack suggest that the flaw required to initiate a crack is fairly large. Furthermore, the size of the cracked region is consistent with the size of the region in which the through-thickness stress exceeds the fracture stress. If the tensile fracture stress does control delamination crack initiation, then delamination becomes more difficult at low temperature since the tensile fracture stress in the ST direction increases. Thus, the increased number of splits indicates that the stress intensity is higher.

The conclusion that the increase in toughness at low temperature is due to factors other than splitting is in general agreement with the literature on controlled-rolled steels (e.g. 15-17) where splitting is associated with an elongated grain structure. In these materials a decrease in upper shelf toughness is often observed relative to alloys that do not split. On the other hand, the steel literature identifies an important role of transverse splitting that is independent of its numerical influence on toughness; because a fully triaxial stress state is not achieved in a split specimen, the ductile-brittle transition is often suppressed. It remains possible that transverse splitting is necessary to preserve a ductile fracture mode of Al-Li alloys, and is hence an essential element in the design of cryogenic alloys. It is also possible that the splitting has a beneficial effect on the fracture toughness at all temperatures. Studies of the effect of splitting on other Al alloys are conflicting (1,18).

Influence of material properties on J_{Ic}. Figure 1 shows the correlation between the variation of toughness and elongation (as well as yield strength and strain hardening rate) with test temperature. For a given yield strength the uniform elongation is determined by the strain hardening rate. Therefore increasing the strain hardening rate should increase the toughness. It is consistent with this hypothesis that both the toughness and the strain hardening rate are higher for 2090-T81 than for 2091-T8.

Analytic theories of elastic-plastic fracture predict that if the fracture mode is unchanged, increases in yield strength, ultimate tensile strength, elongation and strain hardening rate should result in an increased value of J_{Ic}. For example, if we assume strain-controlled fracture and that the relevant microstructural parameters are constant, one standard model becomes (1)

$$J_{Ic} \propto (\varepsilon_f)^{n+1} \sigma_y b$$

where ε_f is the true strain-to-failure, n is the strain hardening rate ($\sigma = k\varepsilon^n$), σ_y is the yield strength and b has dimensions of length. Other models (19) relate K to the square root of the product E x σ_y x n^2 x ε_f. Although the quantitative results differ, when all three parameters increase together, the prediction of increased toughness if the fracture mode is unchanged is the same. These models do not contradict the usual concept that toughness decreases with increasing yield strength, since strain-to-failure and strain hardening rate often decrease concurrently (20). Jata and Starke (5) have suggested that the improved low temperature toughness in 2090 and 8090 can be correlated with a decreased slip band spacing and increased slip band width, as well as with increased E and σ_y. This observation is consistent with the data described here since it implies improved strain hardening at low temperatures. The slip band decohesion failure mechanism postulated by Jata and Starke also implies that the 45° facets on the fracture surface will be longer (5). This increase in crack roughness has been observed (4,5) and may also contribute to the improvement in toughness.

CONCLUSION

The variation of strength, elongation and fracture toughness in two commercial Al-Li alloys 2090-T81 and 2091-T8 has been investigated. In most cases the mechanical properties improve with decreasing temperature. Although the amount of intergranular delamination at cryogenic temperatures is increased over room temperature, the splitting does not seem to be the cause of the improvement in toughness. However, when the fracture mode is unchanged, there is a strong correlation between increasing strain hardening and tensile ductility at low temperatures and improved fracture toughness. When a fracture mode transition does occur, its nature determines the change in fracture toughness.

ACKNOWLEDGEMENT

The authors are grateful to the Aluminum Company of America for research materials, to D. Hoffman, Lawrence Livermore National Laboratory for performing the electron beam welding and to A.J. Sunwoo, Lawrence Berkeley Laboratory, for providing the welding parameters. This study was funded by the Director, Office of Energy Research, Office of Basic Energy Science, Material Sciences Division of the U.S. Department of Energy under Contract No. DE-AC03-76SF00098. J. Glazer was supported by an AT&T Bell Laboratories PhD Scholarship.

REFERENCES

(1) Morris, J.W., Jr. and Glazer, J., International Cryogenic Materials Conference Proceedings, Shenyang, China, 1988, pp. 713-726.

(2) Glazer, J., Verzasconi, S.L., Dalder, E.N.C., Yu, W., Emigh, R.A., Ritchie, R.O. and Morris, J.W. Jr., Adv. Cryo. Eng., Vol. 32, 1986, pp. 397-404.

(3) Dorward, R.C., Scripta Met., Vol. 20, 1986, pp. 1379-1383.

(4) Rao, K.T.V., Hayashigatani, H.F., Yu, W. and Ritchie, R.O., Scripta Met., Vol. 22, 1988, pp. 93-96.

(5) Jata, K.V. and Starke, E.A. Jr., Scripta Met., 1988, Vol. 22, pp. 1553-1556.

(6) Glazer, J. and Morris, J.W., Jr., submitted to Scripta Met.

(7) Glazer, J., Verzasconi, S. L., Sawtell, R. R. and Morris, J.W. Jr., Metall. Trans., Vol. 18A, 1987, pp. 1695-1701.

(8) Glazer, J., Morris, J.W. Jr., Kim, S.A., Austin, M.A. and Ledbetter, H.M., AIAA Journal, Vol. 25, 1987, pp. 1271-1272.

(9) Dew-Hughes, D., Creed, E. and Miller, W.S., Matls. Sci and Tech., Vol. 4, 1988, pp. 106-112.

(10) Rao, K.T.V., Yu, W. and Ritchie, R.O., Metall. Trans., 1989, in press.

(11) D. Webster, Metall.Trans, Vol. 18A, 1987, pp. 2181-2193.

(12) Glazer, J., Nieh, T.G., Wadsworth, J. and Morris, J.W. Jr., Proceedings of Materials Research Society Superplasticity Symposium, Tokyo, Japan, 1988.

(13) Hertzberg, R.W., "Deformation and Fracture Mechanics of Engineering Materials," 2nd edition, Wiley, New York, 1983, p. 355 ff.

(14) Broek, D., "Elementary Engineering Fracture Mechanics," 3rd edition, Martinus Nijhoff, Boston, 1982, p. 199 ff.

(15) Bramfitt, B.L. and Marder, A.R., Metall. Trans., Vol. 8A, 1977, pp. 1263-1273.

(16) Inagaki, H., Z. Metallkde, Vol. 79, 1988, pp. 364-374.

(17) Mintz, B. and Morrison, W.B., Matls. Sci.Tech., Vol. 4, 1988, pp. 719-731.

(18) Verzasconi, S.L. and Morris, J.W. Jr., this conference.

(19) Hahn, G.T. and Rosenfield, A.R., ASTM STP 432, 1968, pp. 5-32.

(20) Embury, J.D and Nes, E., Z. Metallkde, Vol. 64, 1973, pp. 805-812.

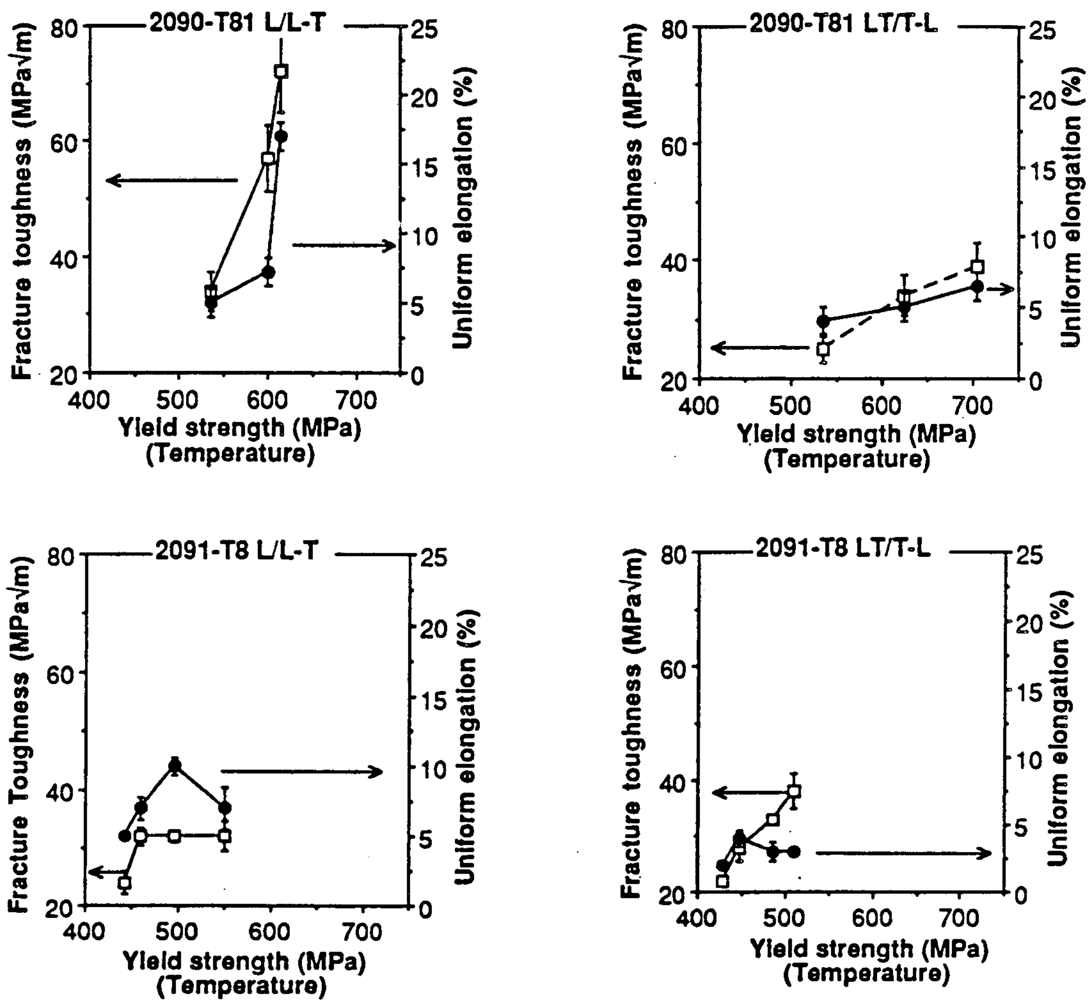

Figure 1. Fracture toughness (open squares) and uniform tensile elongation (closed circles) as a function of yield strength. Increasing strength corresponds to decreasing temperature. Test temperatures (K) are: 2090: 300,77,4; 2091: 300, 200, 77, 4.

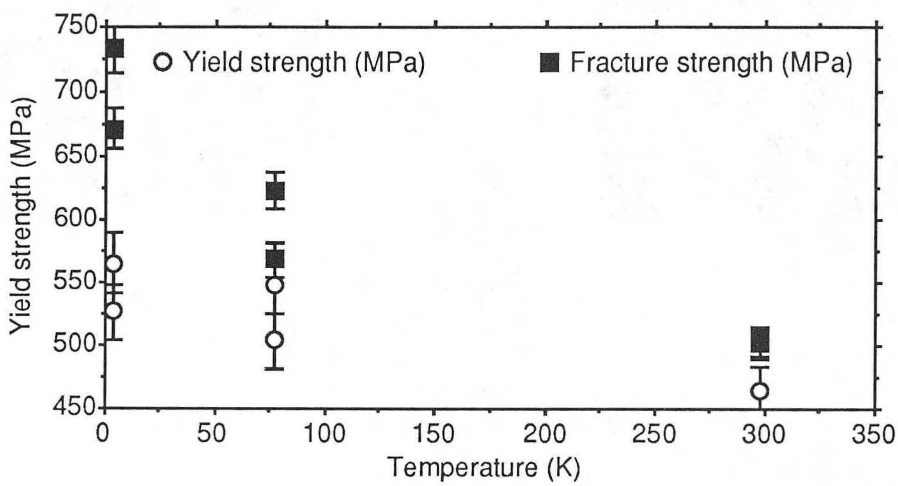

Figure 2. 2090-T81 ST tensile properties as a function of test temperature.

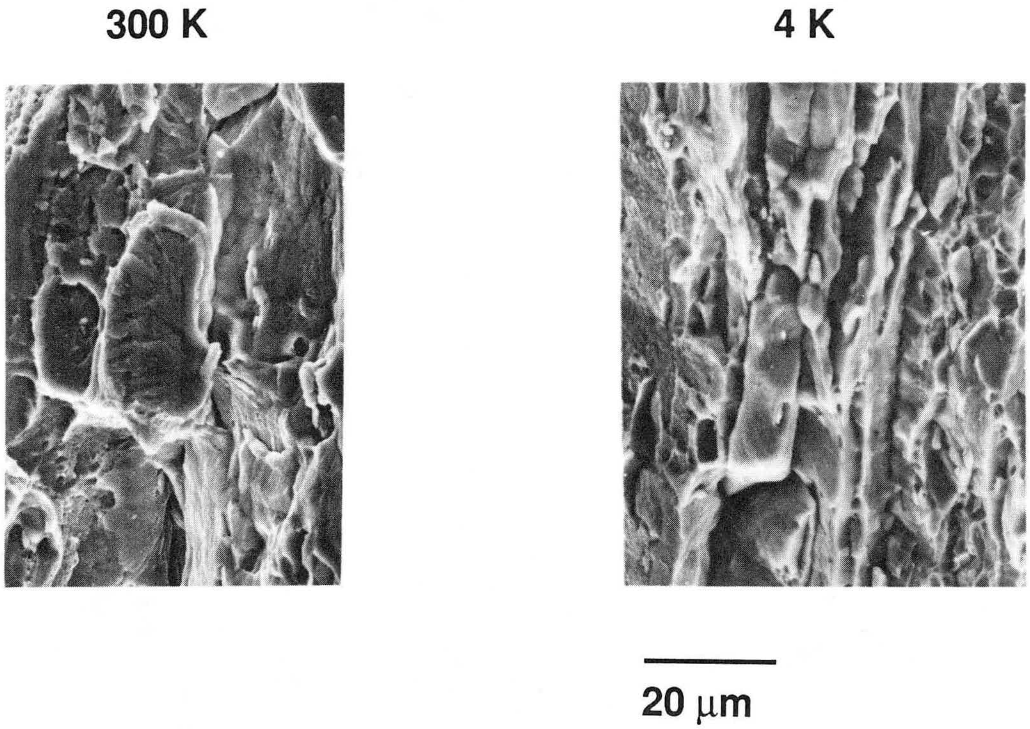

XBB 889-9032

Figure 3. Scanning electron micrographs of 2091-T8 T-L J_{Ic} fracture surfaces.

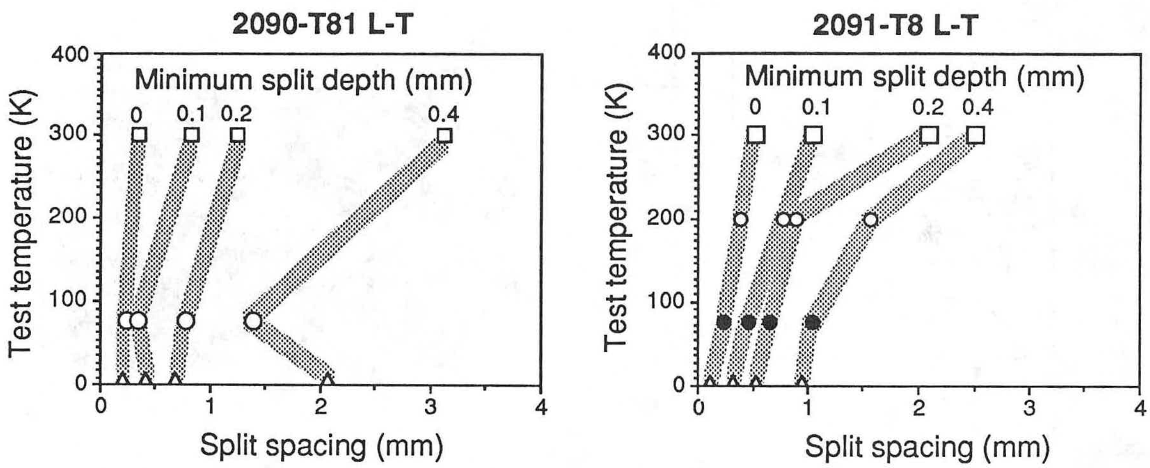

Figure 4. Mean spacing between short-transverse splits as a function of temperature and minimum split depth considered.

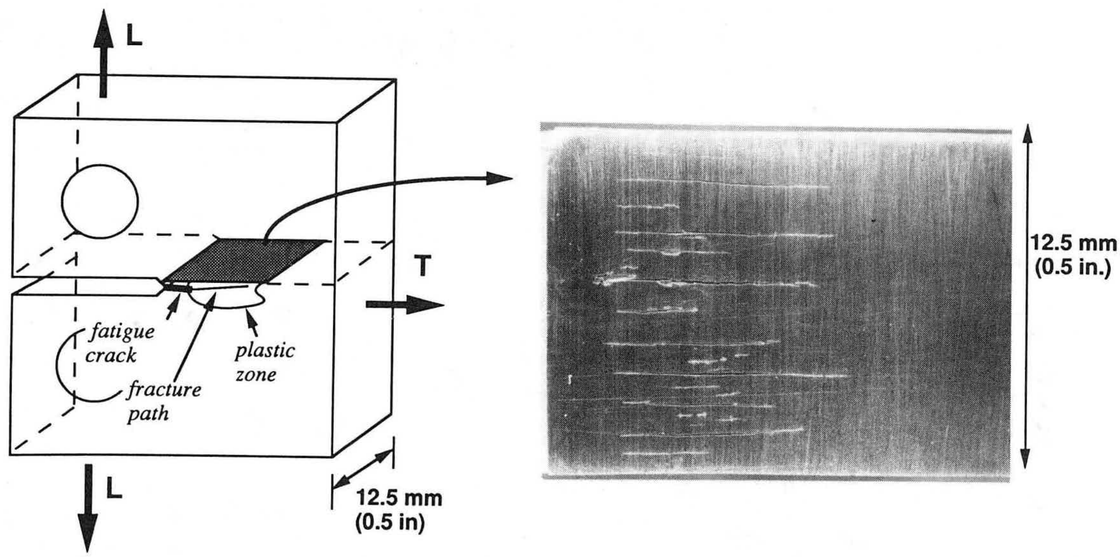

XBB 889-9029

Figure 5. Cross section parallel to the crack plane of 2090-T81 J_{Ic} specimen partially cracked at 77 K. Stripes are delamination cracks.

LAWRENCE BERKELEY LABORATORY
CENTER FOR ADVANCED MATERIALS
1 CYCLOTRON ROAD
BERKELEY, CALIFORNIA 94720